NeuroImage 228 (2021) 117697

Contents lists available at ScienceDirect

NeuroImage

journal homepage: www.elsevier.com/locate/neuroimage

You took the words right out of my mouth: Dual-fMRI reveals intra- and inter-personal neural processes supporting verbal interaction.

M. Salazar[a,b], D.J. Shaw[a,c,*], M. Gajdoš[d], R. Mareček[d], K. Czekóová[a], M. Mikl[d], M. Brázdil[a]

[a] Behavioural and Social Neuroscience Research Group, Central European Institute of Technology (CEITEC), Masaryk University, Kamenice 5, Brno, 62500, Czech Republic
[b] Faculty of Medicine, Masaryk University, Kamenice 5, Brno, 62500, Czech Republic
[c] Department of Psychology, School of Life and Health Sciences, Aston University, Birmingham, B4 7ET, United Kingdom
[d] Multimodal and Functional Neuroimaging Laboratory, Central European Institute of Technology (CEITEC), Masaryk University, Kamenice 5, Brno, 62500, Czech Republic

ARTICLE INFO

Keywords:
Verbal communication
Dual-fMRI
Dynamic causal modeling
Inter-subject correlation

ABSTRACT

Verbal communication relies heavily upon mutual understanding, or common ground. Inferring the intentional states of our interaction partners is crucial in achieving this, and social neuroscience has begun elucidating the intra- and inter-personal neural processes supporting such inferences. Typically, however, neuroscientific paradigms lack the reciprocal to-and-fro characteristic of social communication, offering little insight into the way these processes operate online during real-world interaction. In the present study, we overcame this by developing a "hyperscanning" paradigm in which pairs of interactants could communicate verbally with one another in a joint-action task whilst both undergoing functional magnetic resonance imaging simultaneously. Successful performance on this task required both interlocutors to predict their partner's upcoming utterance in order to converge on the same word as each other over recursive exchanges, based only on one another's prior verbal expressions. By applying various levels of analysis to behavioural and neuroimaging data acquired from 20 dyads, three principal findings emerged: First, interlocutors converged frequently within the same semantic space, suggesting that mutual understanding had been established. Second, assessing the brain responses of each interlocutor as they planned their upcoming utterances on the basis of their co-player's previous word revealed the engagement of the temporo-parietal junctional (TPJ), precuneus and dorso-lateral pre-frontal cortex. Moreover, responses in the precuneus were modulated positively by the degree of semantic convergence achieved on each round. Second, effective connectivity among these regions indicates the crucial role of the right TPJ in this process, consistent with the Nexus model. Third, neural signals within certain nodes of this network became aligned between interacting interlocutors. We suggest this reflects an interpersonal neural process through which interactants infer and align to one another's intentional states whilst they establish a common ground.

1. Introduction

For social interactions to be co-operative, all interactants must act in a manner that complements each other's behaviour and aligns with a shared goal Sebanz, Bekkering, and Knoblich (2006). This is true especially for verbal communication, during which interlocutors engage typically in a joint-action task over reciprocal exchanges in an attempt to establish a common ground, or shared understanding. Inferring the intentional and motivational states of others is fundamental in achieving this (Kestemont et al., 2013), and understanding how the brain supports such inferences during real-time interpersonal co-operation is central to social neuroscience. Historically, however, neuroimaging paradigms have failed to capture the dynamic and bi-directional characteristics of real-world social exchange, thereby offering limited insight into the brain systems that are modulated *online* during interaction (Hari, Henriksson, Malinen, & Parkkonen, 2015; Schilbach, 2010, 2014). To address this, we developed a communicative task in which successful performance requires pairs of interlocutors to co-operate with one another over recursive exchanges to converge on the same word using only their partner's prior verbal expressions. By performing functional magnetic resonance imaging on both interactants simultaneously (dual-fMRI), we then investigated the intra- and inter-personal neural processes associated with the emergence of a common ground, or shared understanding, during verbal communication.

A wealth of neuroscientific research has demonstrated that verbal communication involves the transmission of signals through an indirect chain of interpersonal neural events, through which neural signals

* Corresponding author.
E-mail address: d.j.shaw@aston.ac.uk (D.J. Shaw).

https://doi.org/10.1016/j.neuroimage.2020.117697
Received 27 February 2020; Received in revised form 18 December 2020; Accepted 21 December 2020
Available online 30 December 2020

become coupled between speakers and listeners (e.g., Liu et al., 2017; Silbert et al., 2014; Stephens et al., 2010; Zadbood et al., 2017; see Hasson and Frith, 2016; Hasson et al., 2012). Typically, however, these studies have investigated speech-related neural coupling by measuring the brains of individuals in isolation, offering little information about how these interpersonal processes unfold during real-world conversation. For this reason, and with the advent of second-person neuroimaging Redcay and Schilbach (2019), studies have begun utilizing neuroscientific techniques that afford the measurement of two or more interlocutors' brains while they engaged in dialogue. This has started to reveal discrete patterns of brain-to-brain coupling during different types of verbal and non-verbal exchange (Hirsch et al., 2018; Holper et al., 2013; Nguyen et al. 2020; for reviews see Czeszumski et al., 2020; Scholkmann, Holper, Wolf, & Wolf, 2013). While this "hyperscanning" research has advanced our understanding of the brain processes supporting verbal communication, it has focused primarily on the linear and often uni-directional transfer of information between individuals. Real-world verbal interactions unfold as highly unpredictable, non-linear dynamics, however, whereby interlocutors use back-and-forth exchanges to continuously update their representation of one another's intentional state and adapt their own behaviour accordingly in order to establish a shared understanding.

A large and diffuse collection of brain regions are engaged when we attempt to infer the beliefs and mental states of others, which together form an inter-connected "mentalising" network (Burnett and Blakemore, 2009; Schmälzle et al., 2017); among those reported most consistently are the precuneus (PC), temporo-parietal junction (TPJ), superior temporal sulcus and anterior temporal lobes, the lateral and medial prefrontal cortex (PFC; Bzdok et al., 2012; Dufour et al., 2013; Schurz, Aichhorn, Martin, and Perner, 2013). The TPJ, particularly within the right hemisphere, sits at the nexus of several processing streams wherein external social information converges with that from attention- and memory-related systems (Carter and Huettel, 2013). This position affords the TPJ a central role in re-allocating attention between internal and external signals, distinguishing between self and other representations (Lamm, Bukowski, and Silani, 2016; Uddin, Molnar-Szakacs, Zaidel, and Iacoboni, 2006), coding the reciprocal influence of our own and other's actions (Bhatt, Lohrenz, Camerer, and Montague, 2010; Carter, Bowling, Reeck, and Huettel, 2012), testing and updating our predictions of external events (e.g., Decety & Lamm, 2007), and shaping decision-making processes upstream in the brain. The role of the PC in mentalising remains unclear, but its frequent engagement during mental imagery, self-referential processing and deductive reasoning (Kulakova et al., 2013) implicates it in processes required for behavioural prediction. Within the PFC, the medial aspect appears to represent enduring personal traits Overwalle (2009) while the lateral surface is believed to update the abstract mental representations we hold about others when their behaviour contradicts our expectations (Christoff, Ream, Geddes, and Gabrieli, 2003; Kouneiher, Charron, and Koechlin, 2009; Mende-Siedlecki, Cai, and Todorov, 2013). Together, this network of brain regions might support our moment-by-moment evaluation of others' transient mental states, allowing us to anticipate their behaviour and adapt our own accordingly.

The present study performed an investigation into the neural processes associated with interlocutors' efforts to establish a common ground. To achieve this, we adapted a communicative game for a dual-fMRI experiment – Say the Same Thing (STST), in which pairs of interactants utter words simultaneously in an unconstrained manner over iterative exchanges with the aim of eventually saying the exact same word as one another. Such convergence is achieved more readily if both players say the word that they *expect* their co-player to produce, which requires an inference of their intentional state. At the intra-personal level, then, we hypothesized that brain processes supporting the mental state inference would be engaged on this task as individuals attempt infer and align to their co-player's intentions and/or motivations over successive exchanges in order to predict their partner's upcoming word. With Dynamic Causal Modelling, we also evaluated a prediction of the nexus model of the TPJ (Carter and Huettel, 2013); specifically, that the right TPJ is crucial in establishing a social context, and activity within this region will therefore be observed earlier and serve to modulate activity in other upstream nodes of the mentalising brain network. By imaging the brains of both interlocutors simultaneously, we also examined *inter*-personal brain processes associated with this task. Specifically, by applying an analytical technique capable of identifying patterns of inter-subject correlations in dual-fMRI data (Bilek et al., 2015; Špiláková et al., 2019), we examined whether brain signals become aligned between interlocutors engaged in these co-operative verbal exchanges. We predicted that stronger between-brain alignment would emerge between interacting compared with non-interacting pairs, and greater within-dyad covariance would be associated with a higher rate of convergence on STST.

2. Materials and methods

The neuroimaging data that support the findings of this study are available on request from the corresponding author, DJS. These data are not publicly available because it would compromise the consent of some research participants. All code used in the analysis of these data are available at https://osf.io/su8rd.

2.1. Participants

We recruited 44 right-handed individuals (24 males) from various faculties of Masaryk University, Czech Republic, who were paired into age-matched same-sex dyads. Importantly, paired individuals had never met prior to the day of the experiment; inclusion in the experiment required participants to confirm that they were unfamiliar with the name of the person to whom they were paired. A lack of verbal responses on 10 or more trials over the course of the experiment led to the exclusion of two male pairs. In the final sample of 40 participants (mean age = 26.8 [SD = 3.80, range = 21–36] years; mean intra-dyad difference = 0.7 years), all reported normal or corrected-to-normal vision and no history of neurological diseases or psychiatric diagnosis. All participants provided written informed consent prior to the experimental procedure, which was approved by the Research Ethics Committee of Masaryk University.

2.2. Procedure

The individuals comprising a dyad were introduced to one another for the first time on the day of the experiment, and together asked any questions they had regarding the scanning procedure or task instructions. To ensure their understanding and to familiarize them with one anothers' voices, each dyad played one round (10 trials) of the experimental and control task (see below) outside of the scanner.

The scanning procedure comprised seven rounds (10 trials per round) of the game "Say the Same Thing" (STST), and seven rounds of the "Last Letter Game" (LLG). In STST, a pair of players must each choose a word independently of their co-player and then say their chosen words simultaneously. This is performed over a number of iterations until both players produce the exact same word simultaneously, which, as the name suggests, is the ultimate goal. Such convergence is achieved more readily if both players say the word that they expect their co-player to produce. On all but the first iteration, this can be achieved after careful consideration of the previous word-pair; both players can identify semantic or cultural links between their own and their co-player's previous utterance, and then choose a word that will bridge the words together in the subsequent iteration. Crucially, STST requires both players to limit their choices to words that are likely to be used by the other player – there is little benefit in a player saying a word (e.g., an uncle's name) that is unlikely to be produced by their co-player, even if it

serves to bridge the former word pair (e.g., “Christmas” and “juggling”). In contrast, on each iteration of the LLG, players are required to say a word that begins with the last letter of the word produced previously by their partner. Therefore, in all but the first iteration, the only limitation imposed on a player’s choice is the spelling of their co-player’s previous word. The former served as the experimental condition, while the latter served as a control condition. Although both tasks involve social and verbal processing, they do so to different extents; while the LLG focuses attention on the co-player and word spelling, STST involves a combination of mentalising and semantic processing to choose words that a co-player will interpret as meaningful in the context of a given interaction.

At the beginning of each round, participants were informed what the upcoming task would be by a visual cue. Next, a countdown of 10 seconds was presented to both participants, during which they were instructed to “THINK OF A WORD”. When the timer reached zero, they were cued to “SPEAK” the word they had chosen. Three seconds later, they were cued to “LISTEN” and the word spoken by their partner was played to them during a subsequent interval. The variable duration of recordings introduced inter-trial jitter (428–1383 msec). Under both conditions, on the first trial of each round participants were instructed to choose a word that was independent of any preceding round. From the second trial onwards, participants had to either think of a word that would match what they believed their co-player would say next in an attempt to achieve convergence (STST), or think of a word that started with the last letter of their partner’s previous word (LLG). Sample rounds for both tasks are represented in Fig. 1A. Participants were instructed that if both players said the same word during a STST round, on the next trial they should try to think of an unrelated word to start the game over (see Supporting Information for participant instructions). Two pseudo-randomized sequences of rounds were generated – one being the reverse of the other – that ensured neither condition was played on more than two consecutive rounds without an intervening break. Each sequence was presented to half the sample. After seven rounds, a one-minute break took place. The entire procedure was coded in the Cogent toolbox (www.vislab.ucl.ac.uk/Cogent) for Matlab (v2016b; The MathWorks).

2.3. Behavioural convergence

To obtain a similarity metric for the word pairs uttered on each trial, we employed Word2Vec – a two-layer neural net that “vectorises” words in a text corpus according to their features, and then groups the vectors of similar words together in vectorspace (Mikolov et al., 2013). When features express the context of words, vectors represent semantic similarity. Within Gensim (Řehůřek and Sojka, 2010), we applied latent semantic analysis (Dumais et al., 1988) to *fasttext* (Bojanowski et al., 2017) to obtain a similarity index for each pair of utterances. This allowed us to evaluate if greater similarities were achieved on STST rounds when participants were instructed explicitly to reach convergence, compared to LLG rounds when their task was simply to think of word beginning with last letter of their co-player’s previous utterance.

2.4. Stimuli

A single computer connected to both scanners delivered visual and auditory stimuli to both players simultaneously. The visual cues and countdown timer were presented as white text on a black background. The verbal responses of each player were recorded in MATLAB as stereo wave files, and played back to their co-player using the communication devices built into each scanner. They were recorded in each stereo channel of the computer soundcard separately, and then played back to the co-player through the opposite channel via modified audio-pneumatic memory-foam earplugs. The audio setup is represented in Fig. 1B.

2.5. Imaging protocol

Functional and structural MR data were simultaneously acquired from both players comprising a dyad with two identical 3T Siemens Prisma scanners, each equipped with a 64-channel bird-cage head coil. In a single scanning session, blood-oxygen-level dependent (BOLD) images were acquired with a T_2^*-weighted echo-planar imaging (EPI) sequence with parallel acquisition (i-PAT; GRAPPA acceleration factor = 2; 34 axial slices; TR/TE = 2000/35 msec; flip angle = 60°; matrix = 68 × 68 × 34, 3 × 3 × 4 mm voxels). Axial slices were acquired in an interleaved order, oriented parallel to a line connecting the base of the cerebellum to the base of orbitofrontal cortex to enable whole-brain coverage. To allow voice recordings, functional imaging was performed in a Clustered Temporal Acquisition (CTA) protocol (Schmidt et al., 2008): Through MATLAB, a programmable signal generator (Siglent SDG1025; www.siglent.com) started and stopped 10 s sequences of five volume acquisitions, each separated by a six-second period of silence. Each imaging period captured the duration of the countdown timer on each trial, and silent periods allowed participants to make their verbal response and then to hear the utterance of their partner. This way, participants were unaware of their partner’s word choice, and therefore whether or not they had achieved convergence, until after they had uttered their own word. A schematic of the CTA protocol is presented in Fig. 1C. This resulted in 350 volumes acquired under each condition (7 rounds x 10 trials per round x 5 volumes per trial). A high-resolution T_1-weighted structural MR image was acquired prior to the functional run for localisation and co-registration of the functional time-series (MPRAGE, TR/TE = 2300/2.34 msec; flip angle = 8°; matrix = 240 × 224 × 224, 1 mm^3 voxels).

2.6. Pre-processing

Neuroimaging data were pre-processed with SPM12 (http://www.fil.ion.ucl.ac.uk/spm), which involved spatial realignment and unwarping, slice-time correction, normalization and spatial smoothing. Motion correction was performed using a six-parameter rigid-body transformation, with the first functional scan serving as a reference. Six motion parameters estimated from this realignment process were used as nuisance covariates to account for motion-related variance. Using non-linear transformations (trilinear interpolation; 16 warping iterations), the mean of the motion-corrected time-series was registered to the EPI template in MNI space. Employing analysis parameters that we have used previously for dual-fMRI data (Shaw et al., 2018; Špiláková et al., 2019), images were then smoothed with a 5 mm isotropic Gaussian kernel, and a high-pass filter with 128 s cut-off removed low-frequency drifts. Gradient decay occurring in the CTA protocol caused a systematic artefact in the first three scans of each trial. We corrected the data for this signal decay after each interruption of periodical acquisition with a custom SPM12 script, which calculated the mean decay in voxel intensity and modelled it as a nuisance regressor in the General Linear Modelling procedure (see below) to normalize the affected volumes. As illustrated in Supplementary Figure S1, this proved to be an effective way of modelling the exponential decay in the measured time-series. Data quality after pre-processing was verified using the *mask_explorer* tool (Gajdoš, Mikl, and Mareček, 2016).

2.7. General linear modelling

General linear modelling was performed on the pre-processed time-series using SPM12 (http://www.fil.ion.ucl.ac.uk). The first trial of each round was ignored in this analysis, as these spontaneous choices were assumed to be independent of any prior interaction. The following nine trials of each round were modelled as event-related responses, the onsets of which mirrored the start of the countdown timer. Due to non-systematic desynchronizations between the scanners and the signal generator used

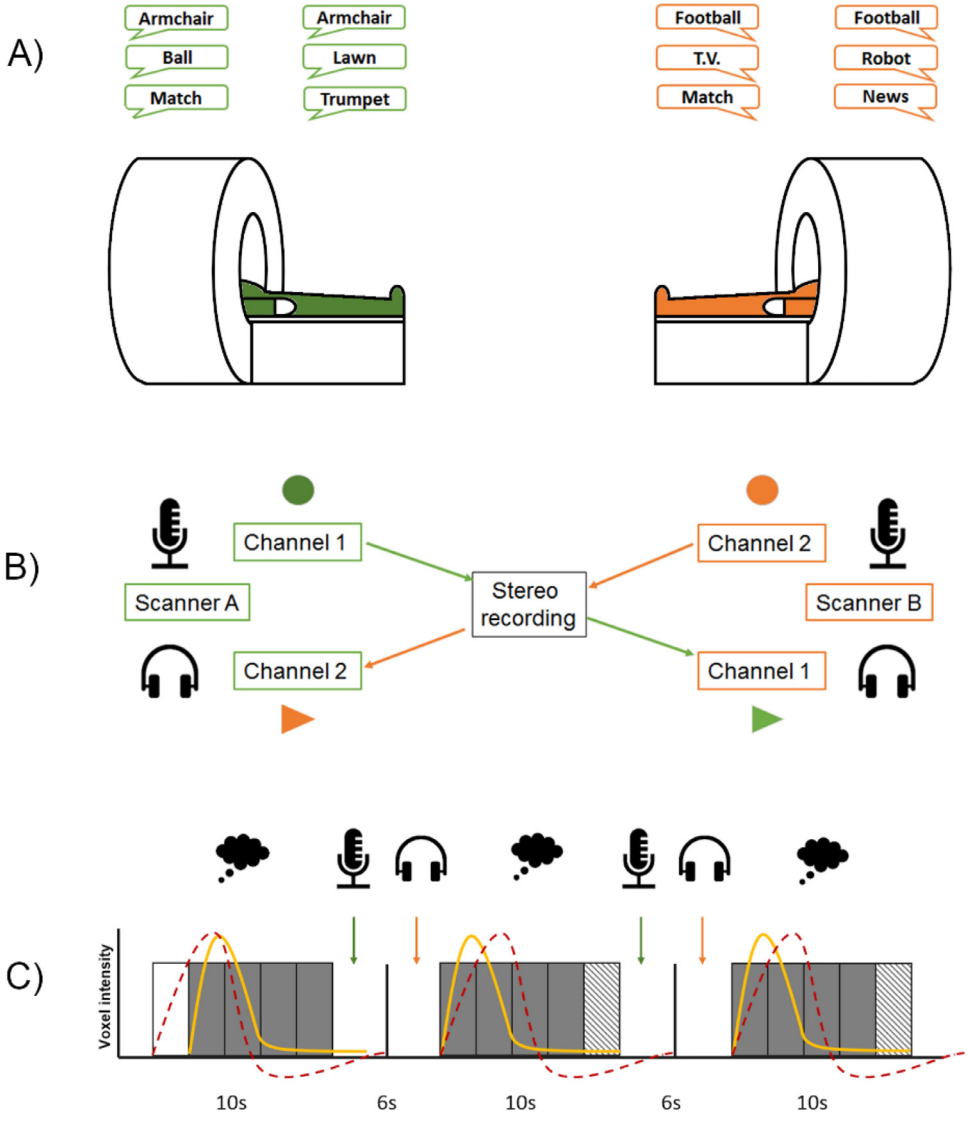

Fig. 1. Experimental setup and procedure. *A*: Pairs of participants were scanned simultaneously whilst they played alternate rounds of STST (*top*) and LLG (*bottom*). *B*: On each round of both conditions, the utterance of each participant was recorded through one stereo channel in their respective scanners and played back for the other participant through the other channel. *C*: Cloud icons represents the 10 second period in which participants planned their next response. Acquisition stopped for six seconds, during which participants' responses were first recorded and then a recording of their partner's response was played-back to them; microphone and headphone icons represent the three seconds for recording and playback of the audio stimuli, respectively. Each grey rectangle represents a volume acquisition lasting two seconds. The empty rectangle represents a missing acquisition due to non-systematic desynchronizations, and striped rectangles represent volumes that were ignored in the GLM procedure to account for any such omissions. Importantly, the hemodynamic response function (red dashed line) during the target planning phase is estimated optimally by ignoring the last of five acquisitions (see text). Yellow curves portray the gradient decay over the course of a round, producing a decrease in the mean voxel intensity.

to start acquisition, the first of the five planned volumes was not acquired on some trials. To account for this, and to estimate the BOLD response during the planning period (uncontaminated by any speech-related response)we removed the last volume of all trials; in this discontinuous CTA protocol, elimination of the first volume would effectively shift the onset of all trials.

As first step, conventional subtraction methods were used to compare the experimental and control condition; we performed a direct contrast of the parametric maps for each condition (STST>LLG) at the first-level, and the resulting contrast images were carried forward to a second-level random-effect one-sample t-test. Secondly, indices of semantic similarity for STST and LLG rounds were introduced as parametric regressors. As the similarity index between two words is expected to influence the degree to which participants would engage in prediction and mental imagery, these regressors were applied to the upcoming trial (i.e. the similarity index of trial 1 was used as a regressor for trial 2). Again, the first trial of every round was ignored in this analysis. For both analyses, the initial cluster determining threshold (CDT) was set at $p < .001$ to reduce the family-wise error (FWE) rate (Eklund et al., 2016). Given the apparent inflation of FWE rates in sparse sampling protocols even with this CDT (Manno et al., 2019), we then implemented FWE correction at the cluster level with $p < .05$.

2.8. Dynamic causal modelling

To evaluate the prediction of the Nexus model (Carter and Huettel, 2013), we performed Dynamic Causal Modelling (DCM) to assess if and how effective connectivity from the right TPJ to other brain regions revealed by the GLM analysis was altered differentially during performance of the STST compared with the LLG task (Friston, Harrison, and Penny, 2003; Stephan et al., 2010). First we conducted volume-of-interest (VOI) analyses on individual's parametric maps of the STST>LLG contrast after a cluster defining threshold (CDT) of $p < 0.05$: Using the MarsBaR toolbox (Brett, Anton, Valabregue, and Poline, 2002), within masks representing discrete functional clusters emerging from the group-level analysis we created spheres of 10 mm radius centred around voxels expressing peak t-values from this contrast. If fewer than 5 voxels survived this CDT within a sphere for any participant, that individual was omitted from further analyses. This yielded usable datasets from 30 participants. We used the first eigenvector as the representative signal, which has been shown to be more efficient than the mean (Gajdoš, Výtvarová, Fousek, Lamoš, and Mikl, 2018).

Modelling these VOIs as network nodes, and the onset of STST rounds as the input (the beginning of the 10 s period in which participants were

instructed to "THINK OF WORD"), we then performed a comprehensive evaluation of all models that met the following logical network conditions: (1) Each node is connected directly with at least one other node; (2) each node is connected at least indirectly to all other nodes; (3) driving stimulus input arrives only at the right TPJ; and (4) the right TPJ has at least one feedforward connection. All of the models meeting these conditions were inverted using DCM (v12.5) implemented in SPM12 (v7487), and then compared using Bayesian Model Comparison (Rigoux, Stephan, Friston, and Daunizeau, 2014; Stephan, Penny, Daunizeau, Moran, and Friston, 2009) implemented in the Variational Bayesian Analysis toolbox of MATLAB (Daunizeau, Adam, and Rigoux, 2014). This analysis evaluated log model evidences to determine the probability that a given model or family of models described the data acquired during STST rounds better than any other model(s). Goodness-of-fit indices can then be estimated based upon the free energy of all compared models, which indicate how well the model(s) fit the observed BOLD time-series; specifically, estimated model frequencies (EMFs) and approximated exceedance probabilities (AEPs). The EMF provides an estimate of the prevalence of each model/family of models in the population. The AEP identifies the relative superiority of one model compared to all others comprising the model space (Penny, Stephan, Mechelli, and Friston, 2004; Stephan, Weiskopf, Drysdale, Robinson, and Friston, 2007); an AEP value of 0.8 indicates that a model is 80% more likely to fit the data better than any other model. Finally, to assess the specificity of any winning model/family of models to data acquired during STST rounds, we again performed Bayesian Model Comparison to compare its fit with the data measured under the LLG condition – that is, with input defined as the onset of LLG rounds.

2.9. Inter-subject correlations

To assess whether our interactive task elicited between-brain alignment, we conducted inter-subject correlation (ISC) analysis informed by group Independent Component Analysis (gICA). A detailed description of this technique is presented in Špiláková et al. (2019), and so we describe only the details of its current implementation in the section that follows.

First, we applied principle component analysis (PCA) to each of the 40 time-series, and subsequently to all the resulting components concatenated into one matrix. This resulted in a set of spatially orthogonal principal components, the number of which was determined by the minimum description length (Sammut and Webb, 2016). Using the GIFT toolbox for MATLAB (v2.0e; mialab.mrn.org/software/gift; Calhoun, Adali, Pearlson & Pekar, 2001), gICA was then performed 20 times on these resulting components using the INFOMAX algorithm to identify those that were expressed reliably and independently of one another at the group level. From the most reliable components, we then identified those that were expressed in individuals' brains along a time-series that corresponded to the STST and/or LLG rounds. Using the results of the PCA, each non-artifactual component was back-reconstructed to each of the 40-input time-series to produce a subject-specific time-course for each component. Multiple regression analyses were then computed to assess the task-specificity of each component: For each subject, the explanatory variables were their back-reconstructed time-course for each independent component and the outcome variable was their unique task design for either the STST or LLG condition. This resulted in two subject-specific β-values for each component, and Bonferroni-corrected paired-samples *t*-tests were conducted to identify task-specific components ($\beta_{STST} > 0$, $\beta_{STST} > \beta_{LLG}$, $\beta_{LLG} > 0$, or $\beta_{LLG} > \beta_{STST}$).

Finally, to examine whether the time-series of BOLD signals covaried between communicating players during STST rounds, for each interacting pair we computed the Pearson correlation between the back-reconstructed time-series for components expressed during the STST condition. The resulting correlation coefficients were transformed to *z*-values, and the median was used as a coefficient of alignment. To determine the significance of the resulting coefficient, we performed a randomization test with 10,000 permutations: in each iteration, we randomly selected pairs among the 38 non-interacting players and computed a median z-transformed coefficient as above. This produced a null distribution of correlations among non-interacting pairs, against which the significance of alignment between each interacting pair was then compared.

3. Results

3.1. Behaviour

One participant failed to provide a word within the response window on four STST rounds, but this did not interrupt the general flow of the task for this pair. One pair chose semantically related words on all LLG rounds, and were therefore omitted from the GLM analysis. For the remaining word pairs, Word2Vec analyses revealed that similarity indices were significantly higher on STST (mean = 0.45 [SD = 0.21]) compared with LLG rounds (mean = 0.25 [SD = 0.13]; t[2632]=28.81, $p < .001$, CI = [.18, .21]). Transcriptions of Czech word pairs, their English translations and similarity indices are provided in Supporting Information.

3.2. Intra-subject brain responses and effective connectivity

Consistent with our hypotheses, the GLM revealed four clusters of increased BOLD response over the course of STST relative to LLG rounds: bilateral TPJ and PC, and right dorso-lateral PFC. Relative increases in BOLD signal were also observed in the anterior/mid-cingulate cortex and medial PFC, but these clusters did not survive FWE-correction. No clusters survived FWE-correction in the reverse contrast (LLG>STST). The parametric modulation analysis revealed that the BOLD response in the precuneus and adjacent posterior cingulate cortex was modulated positively by similarity indices calculated for each word pair - greater word similarity is associated with greater activation in these brain regions. No significant modulation was observed for the LLG condition. These results are illustrated in Fig. 2 and specified in Table 1.

The results of the DCM analysis are shown in Fig. 3. A total of 2432 models met our pre-defined network conditions so we partitioned them into four families, each defined by the conditions shown schematically in Fig. 3A. Of all the inverted models, 1184 belonged to only one of the four families and were carried forward for family comparisons: 112 models in the first (F1), 480 in the second (F2), 224 in the third (F3), and 368 in the fourth (F4). Comparisons of these families performed with VBA identified the best fit between our observed data and the models belonging to family F2, with an EFF of .71 (Fig. 3B). This is confirmed by the free energy over algorithm convergences, which revealed that the observed log evidences are explained better by random-effects generative models than chance alone. Within F2, one model outperformed all others with an AEP of .99. We focus on this specific model herein, illustrated in Fig. 3C. While this optimal model appears to resemble a near fully connected model, one-sample t-tests of connection strengths across all participants (see Table S1) revealed that only the following were reliably strong enough ($p < .05$): reciprocal excitatory connections from left to right (.06 [SE±.02] Hz) and right to left TPJ (.09 [±.03] Hz); excitatory connections from the left (.08 [±.02] Hz) and right TPJ (.09 [±.02] Hz) to the PC, with excitatory feedback from the PC to the left TPJ (.04 [±.01] Hz); and a unidirectional excitatory connection from the right DLPFC to the PC (.03 [±.01] Hz).

When comparing these winning models against data acquired during STST or LLG rounds, however, there was little evidence for any specificity towards the former. As shown in Fig. 3D, while the EFF parameter indicates a slightly better fit of models in F2 to STST measurements, it fell within chance confidence intervals. Further, free energy calculated over VBA iterations revealed that the log model evidences provided no evidence that this family of models fit STST significantly more than measures during LLG rounds).

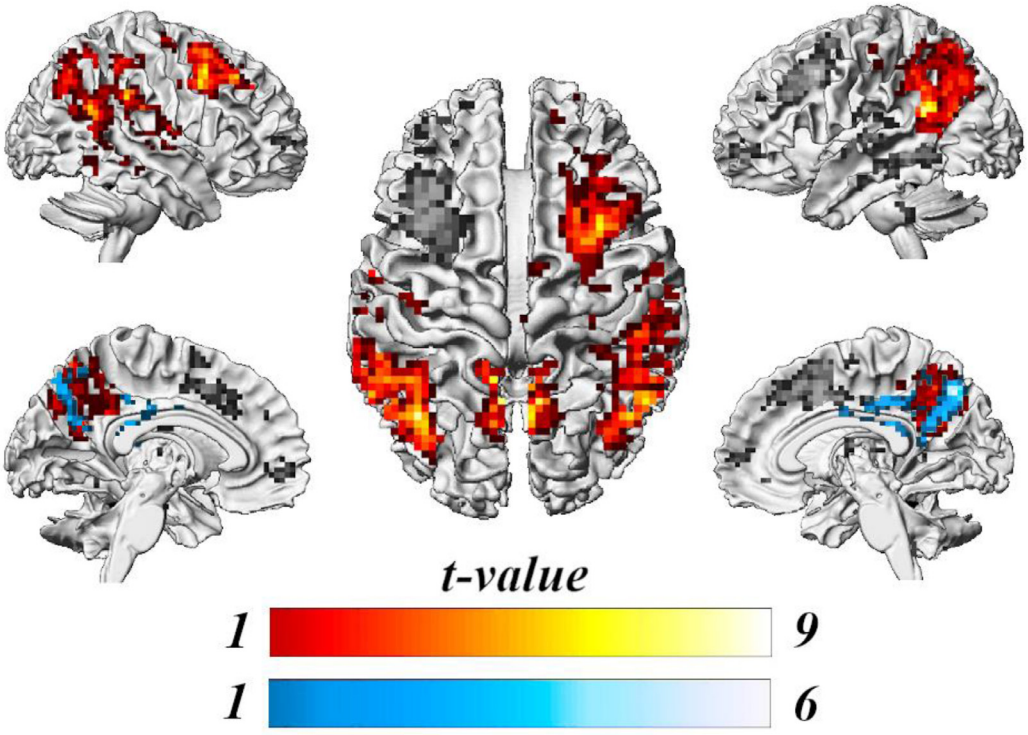

Fig. 2. GLM results. The red scale presents clusters of brain response (p<.001, uncorrected) in the contrast STST>LLG comprising right TPJ and right DLPFC, left TPJ, and bilateral precuneus. Voxels in clusters that did not survive subsequent FWE-correction are rendered in greyscale for ease of interpretation, using xjView toolbox 8 (http://www.alivelearn.net/xjview). The blue scale show the results of the parametric modulation analyses of the STST rounds. Image created in the xjView toolbox 8 (http://www.alivelearn.net/xjview).

Table 1
Clusters of brain response expressing the STST>LLG contrast.

	Label	# Voxels	Peak *t*	x	y	z
STST>LLG	L Angular gyrus	655	7.48	-48	-55	19
			7.07	-39	-52	22
			6.62	-39	-70	37
	R Lateral occipital cortex	626	6.75	48	-67	34
			6.26	51	-13	13
			6.25*	42	-55	22
	L Precuneus	843	8.50	-3	-58	43
			7.29	-3	-64	52
			6.60	-9	-46	34
	R Middle frontal gyrus	439	6.77	30	11	58
			5.65	36	14	43
			5.20	30	38	40
Parametric Modulation	R Posterior cingulate cortex	253	5.24	3	-31	43
			5.23	9	-46	37
			4.95	-6	-34	40
	L Precuneus	114	4.41	-9	-73	37
			4.37	-9	-73	25
			3.61*	-9	-73	52
	R Precuneus	143	5.16	15	-67	31
			5.02	18	-70	43
			4.98	6	-70	46

Note: All clusters survived family-wise error correction (p_{FWE}<.05). Coordinates (mm) are given in the standard space of the Montreal Neurological Institute template, and labels correspond to those specified in Harvard-Oxford Cortical Structural Atlas. Grey rows indicate the coordinates around which spheres were centred for VOIs. TPJ=temporo-parietal junction, PFC=dorso-lateral prefrontal cortex; L/R=left/right.

3.3. Inter-subject neuroimaging data

Initial data reduction of the 40-input time-series with PCA identified a set of 59 spatially orthogonal principal components, which were then fed into 20 iterations of gICA. The resulting estimates were compared using ICASSO, which confirmed that all 59 components achieved very high indices of cluster quality (I_q=.97–.99). We then identified components reflecting artefactual signals (e.g., head motion, heart-beat, acquisition artefacts) using principles underpinning an automated classifier (Bhaganagarapu et al., 2013); specifically, if a given component expressed a narrow range of high power in temporal frequencies beyond 0.08 Hz, and/or a large extent of its spatial pattern lay within periph-

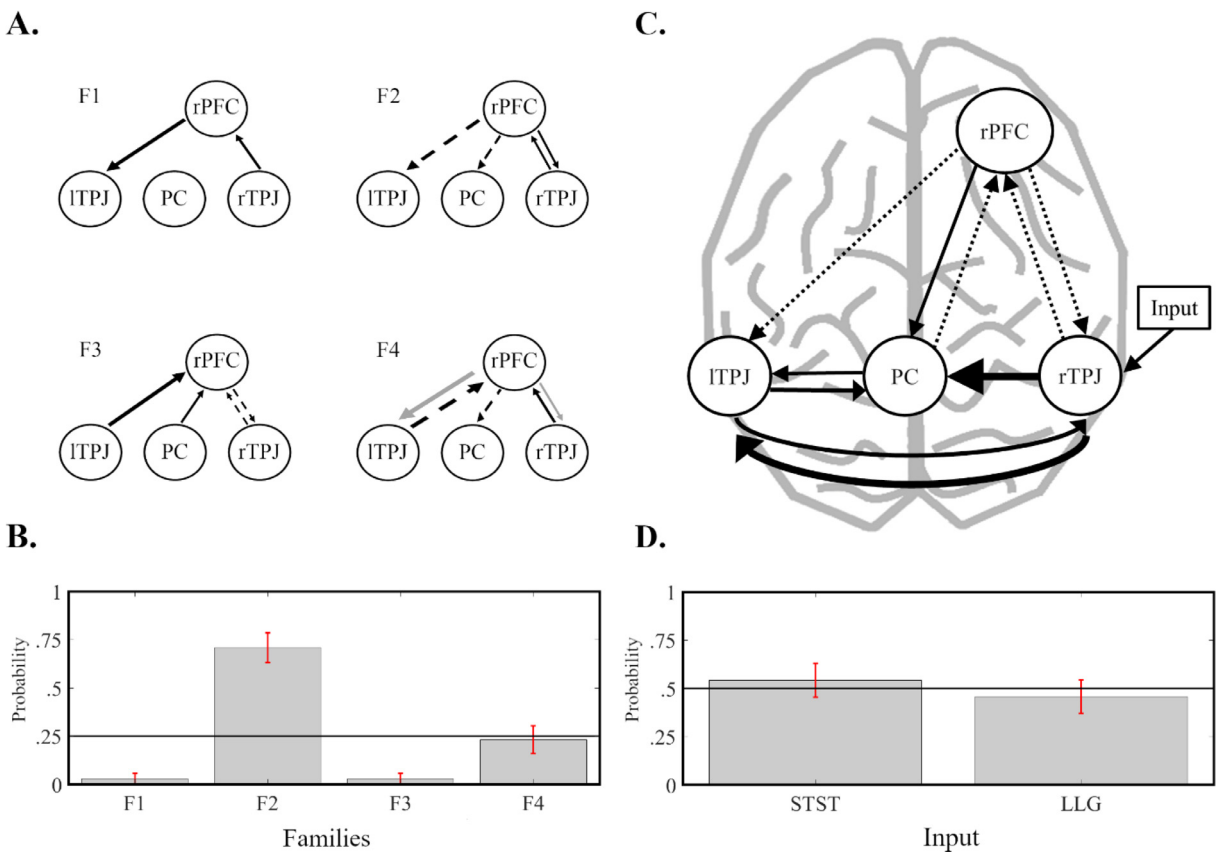

Fig. 3. DCM results. A: Schematics of the parameters defining each family of models. Straight lines indicate strictly necessary connections, dashed arrows represent optional connections, and dotted arrows are mutually exclusive connections. For all families, the right TPJ served as the input node. *B*: Estimated Family Frequencies from a comparison between all four families fitted to data acquired during STST rounds, illustrating that F2 is estimated to be significantly more prevalent in the population (the dashed horizontal line represent the 'null' frequency profile over all models). *C*: Best fitting model of the winning family (F2). Dashed lines illustrate connections with non-significant strength. Solid line thickness represents the strength of connections (see text for details). D: Estimated Family Frequencies following the comparison of fit for F2 against STST or LLG data, illustrating no significant difference. *Abbreviations*: rPFC=right dorso-lateral prefrontal cortex, l/rTPJ=left/right temporo-parietal junction, PC=precuneus.

eral and/or ventricular areas of the brain. This revealed 25 artefactual components that were excluded from subsequent analyses (see Figure S2). From the back-reconstructed time-series of these remaining 32 components, Bonferroni-corrected paired-samples *t*-tests identified only one that demonstrated any significant task-specificity; namely, a component for which the β value was significantly greater than zero across all players for STST rounds (mean = .21 [SD=.33]; t[39] = 4.01, p_{corr}=.01), but not LLG rounds (mean = .13 [SD = .34]; t[39] = 2.49, p_{corr}=.550). This component, illustrated in see Fig. 4, comprised bilateral medial and dorso-lateral PFC, right posterior superior temporal sulcus, and bilateral inferior parietal lobule. Pearson correlations revealed that the subject-specific time-series of this component correlated positively between interacting individuals (median r = .18; range = -.07–.47), and significantly more strongly than for non-interacting subjects paired randomly (p = .012; see Fig. 4C).

Finally, we assessed whether the strength of neural alignment expressed within this component was associated with the degree of semantic convergence achieved on each round of the STST task. To do so, we first concatenated all the functional volumes acquired during the STST and LLG rounds separately. For each pair, we then calculated a coefficient of alignment specific to each condition, before performing a Fisher *r*-to-*z* transformation of the alignment coefficient. Importantly, this revealed that the strength of alignment was similar on both types of rounds (.12 [.23] *vs.* .11 [.19]; t[36]= -.09, p = .930). We then performed a Pearson correlation on z-transformed alignment coefficients and the mean semantic similarity achieved across all STST rounds. This revealed that the degree of inter-brain alignment was unrelated to performance on the task (r = -0.06, p = .802).

4. Discussion

This study explored the brain processes associated with interlocutors' efforts to establish a common ground during verbal communication, both at the intra- and inter-personal level. We achieved this by measuring the brain responses of interactants engaged co-operatively in Say the Same Thing (STST) – a joint-action game of verbal exchange, whereby each player must attempt to predict their co-player's next spoken word based only on their previous utterances. Assessing brain responses across the whole sample, this game elicited strong responses within the bilateral temporo-parietal junction (TPJ), the precuneus (PC), and right dorso-lateral prefrontal cortex (PFC). Given the frequent engagement of these brain regions in tasks requiring mentalising (see review by Schurz, Radua, Aichhorn, Richlan, and Perner, 2014), we interpret their involvement to reflect the effort of interlocutors to infer and align with their co-player's intentions in order to achieve common ground. Consistent with this interpretation, a parametric modulation analysis revealed that the degree of similarity achieved on each round of STST was associated with the magnitude of response in the PC. Furthermore, our modelling of effective connectivity supports the hypothesis that the right TPJ exerts a modulatory influence over this interconnected network, consistent with its purported role in the re-allocation of attention from self- to other-representations during social decision making

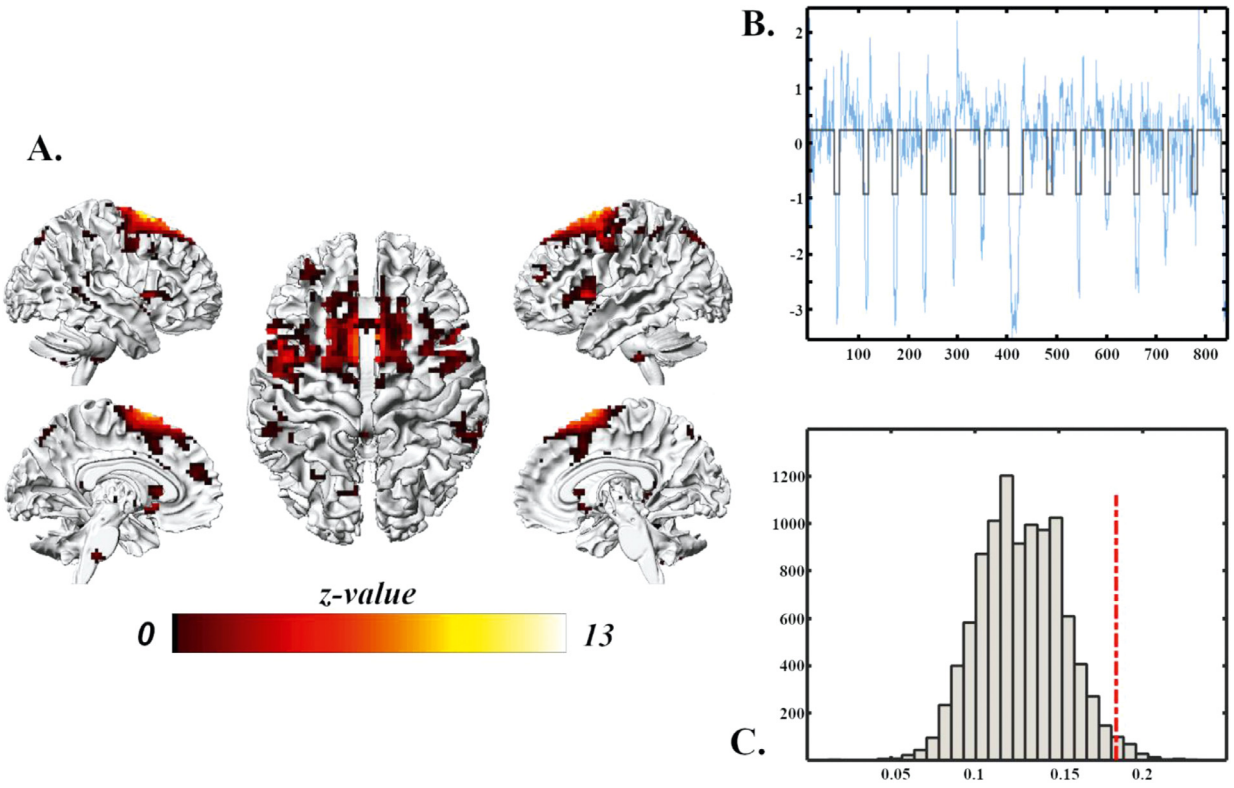

Fig. 4. Results of inter-subject neuroimaging analyses. *A:* Spatial distribution of the only component emerging from the group Independent Component Analysis (gICA) that was aligned significantly ($p<.05$) with the time-series of STST rounds. *B:* Time-series expressing the probability of response within the component in each volume at the group level (*blue*), presented with an example time-course of control and experimental rounds. *C:* Null distribution of median correlation coefficients among all non-interacting pairs, with the median coefficient of interacting pairs presented as a red line.

(Carter and Huettel, 2013; Decety and Lamm, 2007). Inter-subject correlations revealed a pattern of inter-brain alignment that was stronger between interacting compared with non-interacting individuals, encompassing bilateral dorso-lateral and dorso-medial PFC, STS and inferior frontal gyrus (IFG). This was unspecific to the nature of the interaction, however, and, contrary to our hypothesis, unrelated to performance on the STST task.

We propose that the set of neural responses elicited during STST form a system through which interactants' attention is reallocated (Geng and Vossel, 2013; Vossel, Geng, and Fink, 2014) to facilitate reciprocal choices when attempting to establish a common ground during conversation (Vanlangendonck, Willems, and Hagoort, 2018). This is supported partly by the functional and anatomical connectivity profile among these brain regions during social information processing (Burnett and Blakemore, 2009; Jung, Cloutman, Binney, and Lambon Ralph, 2017; Schmälzle et al., 2017; see also Zhang and Li, 2013). Given its overlap with language-related regions, it is perhaps unsurprising that the left TPJ is engaged when choosing a specific term or phrase for referral. Operating in concert with a wider network, the right dorso-lateral PFC also appears to play an important role in this planning process; this cortical region is engaged more during the processing of semantic compared with phonological aspects of words (McDermott, Petersen, Watson, and Ojemann, 2003), and facilitatory stimulation of this brain site improves performance in the Verb Generation Task (Erickson et al., 2017). Two transcranial magnetic stimulation (TMS) studies provide further insights into the potential social role of the dorso-lateral prefrontal cortices in our communicative task: disrupting neural activity within this brain region reduces participants' rejections of unfair offers on the Ultimatum Game (Knoch, Pascual-Leone, Meyer, Treyer, and Fehr, 2006), a task on which choices reflect reciprocal tendencies (Shaw et al., 2018; 2019). Taken together, past studies suggest that, during a verbal joint-action task like STST, activity in the right dorso-lateral PFC might support reciprocal word choices guided by the prior behaviour of an interaction partner.

The interpretation presented above accords with the pattern of effective connectivity we observed with DCM. Connection strengths from and between right and left TPJ are stronger than those coming from PC and right dorso-lateral PFC. This might indicate variability in the strategies employed on the STST task; on some rounds, participants may engage in deductive reasoning and mental imagery processes that recruit the PC (Kulakova et al., 2013). Indeed, our parametric analysis revealed that the involvement of the PC was greater when pairs achieved greater similarity in their utterances. On other rounds, they may opt instead for reciprocal over strategic choices that engage the right dorso-lateral PFC (Smittenaar et al., 2013). In contrast, the stronger influence of bilateral TPJ throughout the task may reflect its role in processes necessary for task performance; for example, meta-analytic data imply a role of the TPJ in reallocating attention between representations of the self and others (Murray, Schaer, and Debbané, 2012; van Veluw and Chance, 2014), and positions this brain region within dissociable functional networks associated with internal processes (e.g., memory and attention) and those involved in the processing of social stimuli (Bzdok et al., 2012). Furthermore, meta-analyses highlight overlapping activations within the TPJ during attention reorienting and mental state inferences (Krall et al., 2015; Scholz, Triantafyllou, Whitfield-Gabrieli, Brown, and Saxe, 2009). In this light, achieving a common ground during verbal exchange are likely to draw on processes performed by TPJ, such as efficient switching between self- and other-representations (Lamm et al., 2016), shifting attention between internal and external signals (Krall et al., 2015), and coding the reciprocal influences of our and other's actions (Bhatt et al., 2010; Carter et al., 2012).

Importantly, however, the family of models emerging from our DCM analyses showed no specificity to STST rounds; they fit equally well to data acquired during the Last Letter Game (LLG). Although the component emerging from the group ICA regressed onto the timings of the STST but not LLG rounds, inter-brain alignment within that component was also task-unspecific. The fact that inter-subject correlations within the medial PFC were equally as strong during exchanges on STST and LLG rounds might indicate that both tasks place similar demands on neural systems supporting reciprocal adaptation or linguistic processes during verbal exchanges, revealing a potential limitation in our choice of control condition. Consistent with the latter possibility, meta-analytic data have shown that speech production and comprehension engage dorso-medial PFC. This is true also for the IFG – another brain region encompassed by the component expressed during STST rounds Adank (2012). Interestingly, however, between-brain alignment has been reported in other non-verbal tasks within the dorso-medial PFC (Shaw et al., 2018; Špiláková et al., 2019) and IFG (Koike et al., 2015; Liu et al., 2011; Saito et al., 2010). It is also noteworthy that the only brain region in which responses were associated with the performance on the STST task was the precuneus – an area that did not feature in the component emerging from the group ICA. Perhaps, then, the multi-level analyses we have performed captured two different brain responses: the model-free technique of group ICA revealed those that are common to various forms of social interaction, while the model-drivem GLM analysis identified those specific to the establishment of common ground. Future studies should investigate the nature of neural coupling with these specific cortical areas during social interaction by extending our paradigm with other non-verbal control conditions.

A valuable contribution of our study is the introduction of an interactive task capable of eliciting reliable brain responses during naturalistic conversation – one that permits an investigation of the neural processes that unfold as interlocutors choose verbal responses in complete freedom, as opposed to the constraints imposed typically by experimental paradigms used in social neuroscience research (Schilbach et al., 2013). This second-person approach provides a more accurate simulation of minimalistic conversation Redcay and Schilbach (2019): A tacit agreement emerges naturally as the flow of conversation follows what we believe our interaction partner does or does not know Grice (1989), using what we have learnt about them over successive exchanges (Shintel and Keysar, 2009). In realizing this experimental paradigm, we have also demonstrated the utility of clustered temporal acquisition protocols (Schmidt et al., 2008; Zaehle et al., 2007) coupled with dual-channel audio setups for (dual-)fMRI investigations of real-world verbal communication. Given recent advances in active noise cancelation, the quality of audio stimuli should now be sufficient to allow for more complex communication than the short utterances used in this experiment.

4.1. Conclusion

Using a communicative joint-action task, we have revealed both intra- and inter-personal brain processes that appear to support interlocutors in aligning within the same semantic space during verbal communication, and thereby establishing a common ground. Our data present a potential neurophysiological model that facilitates the co-adaptive choices made in communicative environments wherein interlocutors influence one another reciprocally in a dynamic and bidirectional manner. Our results also lend further evidence for the important role of the right TPJ in this process, consistent with its purported role in processes required for, but not restricted to, social cognition and behaviour, such as the reallocation of attention between internal and external signals. We propose that the dorso-lateral PFC should be a target for further exploration in social neuroscience, as its involvement in our task suggests its crucial role in the real-time co-adaptation that characterises co-operative social exchanges.

Author statement

Miguel Salazar: Conceptualization, Methodology, Investigation, Writing – Original Draft, Visualization. **Daniel Shaw:** Supervision, Funding acquisition, Writing – Review & Editing. **Martin Gajdoš:** Methodology, Formal analysis, Data Curation, Software. **Radek Mareček:** Methodology, Formal analysis, Data Curation, Software. **Kristína Czekóová:** Project administration, Writing – Review & Editing. **Michal Mikl:** Software, Resources. **Milan Brazdil:** Writing – Review & Editing.

Data code availability

The neuroimaging data that support the findings of this study are available on request from the corresponding author, DJS. These data are not publicly available because it would compromise the consent of some research participants. All code used in the analysis of these data are available at https://osf.io/su8rd

Acknowledgements

We would like to thank Pavel Smrž for his assitance in the Word2Vec analyses. This work was supported financially by the Ministry of Education, Youth and Sports of the Czechia under the Project CEITEC 2020 (LQ1601) and Czech Science Foundation (project no. GA16-18261S). We acknowledge the core facility MAFIL of CEITEC supported by the MEYS CR (LM2018129 Czech-BioImaging).

Supplementary materials

Supplementary material associated with this article can be found, in the online version, at doi:10.1016/j.neuroimage.2020.117697.

References

Adank, P., 2012. The neural bases of difficult speech comprehension and speech production: two activation likelihood estimation (ALE) meta-analyses. Brain Lang. 122 (1), 42–54. doi:10.1016/j.bandl.2012.04.014.

Bhaganagarapu, K., Jackson, G.D., Abbott, D.F., 2013. An automated method for identifying artifact in Independent Component Analysis of resting-state fMRI.. Frontiers in Human Neuroscience 7 (343), 1–16. doi:10.3389/fnhum.2013.00343.

Bhatt, M.A., Lohrenz, T., Camerer, C.F., Montague, P.R., 2010. Neural signatures of strategic types in a two-person bargaining game. Proc. Natl. Acad. Sci. 107 (46), 19720–19725. doi:10.1073/pnas.1009625107.

Bilek, E., Ruf, M., Schäfer, A., Akdeniz, C., Calhoun, V.D., Schmahl, C., Meyer-Lindenberg, A., 2015. Information flow between interacting human brains: Identification, validation, and relationship to social expertise. Proc. Natl. Acad. Sci. 112 (16), 5207–5212.

Brett, M., Anton, J.-L.L., Valabregue, R., Poline, J.-B., 2002. Region of interest analysis using the MarsBar toolbox for SPM 99. Neuroimage 16 (2), S497. doi:10.1016/S1053-8119(02)90010-8.

Burnett, S., Blakemore, S.-J., 2009. Functional connectivity during a social emotion task in adolescents and in adults. Eur. J. Neurosci. 29 (6), 1294–1301. doi:10.1111/j.1460-9568.2009.06674.x.

Bzdok, D., Schilbach, L., Vogeley, K., Schneider, K., Laird, A.R., Langner, R., Eickhoff, S.B., 2012. Parsing the neural correlates of moral cognition: ALE meta-analysis on morality, theory of mind, and empathy. Brain Struct. Funct. 217 (4), 783–796. doi:10.1007/s00429-012-0380-y.

Carter, R.M., Bowling, D.L., Reeck, C., Huettel, S.A., 2012. A distinct role of the temporal-parietal junction in predicting socially guided decisions. Science 336 (6090), 109–111. doi:10.1126/science.1219681.

Carter, R.M., Huettel, S.A., 2013. A nexus model of the temporal-parietal junction. Trends Cogn. Sci. 17 (7), 328–336. doi:10.1016/j.tics.2013.05.007.

Christoff, K., Ream, J.M., Geddes, L.P.T., Gabrieli, J.D.E, 2003. Evaluating self-generated information: anterior prefrontal contributions to human cognition. Behav. Neurosci. 117 (6), 1161–1168. doi:10.1037/0735-7044.117.6.1161.

Czeszumski, A, Eustergerling, S, Lang, A, Menrath, D, Gerstenberger, M, Schuberth, S, Schreiber, F, Rendon, ZZ, König, P, 2020. Hyperscanning: a valid method to study neural inter-brain underpinnings of social interaction. Front. Hum Neurosci. 14, 39.

Daunizeau, J., Adam, V., Rigoux, L., 2014. VBA: a probabilistic treatment of nonlinear models for neurobiological and behavioural data. PLoS Comput. Biol. 10 (1). doi:10.1371/journal.pcbi.1003441.

Decety, J., Lamm, C., 2007. The role of the right temporoparietal junction in social interaction: how low-level computational processes contribute to meta-cognition. The Neuroscientist 13 (6), 580–593. doi:10.1177/1073858407304654.

Dufour, N, Redcay, E, Young, L, Mavros, PL, Moran, JM, Triantafyllou, C, Gabrieli, JDE, Saxe, R, 2013. Similar brain activation during false belief tasks in a large sample of adults with and without Autism Gilbert S,. ed. PLoS One 8, e75468. doi:10.1371/journal.pone.0075468, Available at:Accessed July 27, 2020.

Dumais, S.T., Furnas, G.W., Landauer, T.K., Deerwester, S., Harshman, R., 1988. Using latent semantic analysis to improve access to textual information. In: Proceedings of the SIGCHI Conference on Human Factors in Computing Systems, pp. 281–285.

Bojanowski, P., Grave, E., Joulin, A., Mikolov, T., 2017. Enriching word vectors with subword information. Trans. Ass. Comput. Linguistics 5, 135–146.

Eklund, A., Nichols, T.E., Knutsson, H., 2016. Cluster failure: Why fMRI inferences for spatial extent have inflated false-positive rates. Proceedings of the National Academy of Sciences 28, 7900–7905. doi:10.1073/pnas.1602413113.

Erickson, B., Rosen, D., Mirman, D., Hamilton, R.H., Kim, Y.E., Kounios, J., 2017. tDCS of the right DLPFC increases semantic distance of responses on the verb generation task. Brain Stimulation 10 (1), e10. doi:10.1016/j.brs.2016.11.049.

Friston, K.J., Harrison, L., Penny, W., 2003. Dynamic causal modelling. Neuroimage 19 (4), 1273–1302. doi:10.1016/S1053-8119(03)00202-7.

Gajdoš, M., Mikl, M., Mareček, R., 2016. Mask_explorer: a tool for exploring brain masks in fMRI group analysis. Comput. Methods Programs Biomed. 134, 155–163. doi:10.1016/j.cmpb.2016.07.015.

Gajdoš, M., Výtvarová, E., Fousek, J., Lamoš, M., Mikl, M., 2018. Robustness of representative signals relative to data loss using atlas-based parcellations. Brain Topogr. 31 (5), 767–779. doi:10.1007/s10548-018-0647-6.

Geng, J.J., Vossel, S., 2013. Re-evaluating the role of TPJ in attentional control: contextual updating? Neurosci. Biobehav. Rev. 37 (10), 2608–2620. doi:10.1016/j.neubiorev.2013.08.010.

Grice, H.P., 1989. Studies in the Way of Words. Hardvard University Press, Cambridge MA.

Hari, R., Henriksson, L., Malinen, S., Parkkonen, L., 2015. Perspective centrality of social interaction in human brain function. Neuron 88, 181–193. doi:10.1016/j.neuron.2015.09.022.

Hasson, U., Frith, C.D., 2016. Mirroring and Beyond: Coupled Dynamics as a Generalized Framework for Modelling Social Interactions.. Philosophical Transactions of the Royal Society B: Biological Sciences 371, 20150366. doi:10.1098/rstb.2015.0366.

Hasson, U., Ghazanfar, A.A., Galantucci, B., Garrod, S., Keysers, C., 2012. Brain-tobrain coupling: a mechanism for creating and sharing a social world. Trends in Cognitive Sciences 16 (2), 114–121. doi:10.1016/j.tics.2011.12.007.

Hirsch, J, Noah, JA, Zhang, X, Dravida, S, Ono, Y, 2018. A cross-brain neural mechanism for human-to-human verbal communication. Soc Cogn Affect Neurosci 13, 907–920.

Holper, L, Goldin, AP, Shalóm, DE, Battro, AM, Wolf, M, Sigman, M, 2013. The teaching and the learning brain: a cortical hemodynamic marker of teacher-student interactions in the Socratic dialog. Int. J. Educ. Res. 59, 1–10.

Jung, J., Cloutman, L.L., Binney, R.J., Lambon Ralph, M.A., 2017. The structural connectivity of higher order association cortices reflects human functional brain networks. Cortex 97, 221–239. doi:10.1016/J.CORTEX.2016.08.011.

Kestemont, J., Vandekerckhove, M., Ma, N., Van Hoeck, N., Van Overwalle, F., 2013. Situation and person attributions under spontaneous and intentional instructions: an fMRI study. Soc. Cogn. Affect. Neurosci. 8 (5), 481–493. doi:10.1093/scan/nss022.

Knoch, D., Pascual-Leone, A., Meyer, K., Treyer, V., Fehr, E., 2006. Diminishing reciprocal fairnes by disrupting the right prefrontal cortex. Science 314 (5800), 829–832. doi:10.1126/science.1082976.

Koike, T., Tanabe, H.C., Okazaki, S., Nakagawa, E., Sasaki, A.T., Shimada, K., Sadato, N., 2015. Neural substrates of shared attention as social memory: a hyperscanning functional magnetic resonance imaging study. Neuroimage doi:10.1016/j.neuroimage.2015.09.076.

Kouneiher, F., Charron, S., Koechlin, E., 2009. Motivation and cognitive control in the human prefrontal cortex. Nat. Neurosci. 12 (7), 939–945. doi:10.1038/nn.2321.

Krall, S.C., Rottschy, C., Oberwelland, E., Bzdok, D., Fox, P.T., Eickhoff, S.B., Konrad, K., 2015. The role of the right temporoparietal junction in attention and social interaction as revealed by ALE meta-analysis. Brain Struct. Funct. 220 (2), 587–604. doi:10.1007/s00429-014-0803-z.

Kulakova, E., Aichhorn, M., Schurz, M., Kronbichler, M., Perner, J., 2013. Processing counterfactual and hypothetical conditionals: an fMRI investigation. Neuroimage 72, 265–271. doi:10.1016/j.neuroimage.2013.01.060.

Lamm, C., Bukowski, H., Silani, G., 2016. From shared to distinct self-other representations in empathy: evidence from neurotypical function and socio-cognitive disorders. Philos. Trans. Royal Soc. B (1686) 371. doi:10.1098/rstb.2015.0083.

Liu, T., Saito, G., Chenhui, L., Saito, H., 2017. Inter-brain network underlying turn-based cooperation and competition: A hyperscanning study using near-infrared spectroscopy. Scientific Reports 7, 8684. doi:10.1039/s41598-017-09226-w.

Liu, T., Saito, Hirofumi., Oi, Misato, 2011. The Effect of the Presence of An Observer on Prefrontal Cortex during a Driving Video Game: A Near-Infrared Spectroscopy Study. i-Perception 2, 873. doi:10.1068/ic873.

Manno, F.A.M., Fernandez-Ruiz, J., Manno, S.H.C., Cheng, S.H., Lau, C., Barrios, F.A, 2019. Sparse sampling of silence type I errors with an emphasis on primary auditory cortex. Front. Neurosci. 13, 516. doi:10.3389/fnins.2019.00516.

McDermott, K.B., Petersen, S.E., Watson, J.M., Ojemann, J.G., 2003. A procedure for identifying regions preferentially activated by attention to semantic and phonological relations using functional magnetic resonance imaging. Neuropsychologia 41 (3), 293–303. Retrieved from http://www.ncbi.nlm.nih.gov/pubmed/12457755 .

Mende-Siedlecki, P., Cai, Y., Todorov, A., 2013. The neural dynamics of updating person impressions. Soc. Cogn. Affect. Neurosci. 8 (6), 623–631. doi:10.1093/scan/nss040.

Mikolov, T., Chen, K., Corrado, G., Dean, J., 2013. Efficient estimation of word representations in vector space. Proceedings of ICLR Workshops Track. https://arxiv.org/abs/1511.06051.

Murray, R.J., Schaer, M., Debbané, M., 2012. Degrees of separation: a quantitative neuroimaging meta-analysis investigating self-specificity and shared neural activation between self- and other-reflection. Neurosci. Biobehav. Rev. 36 (3), 1043–1059. doi:10.1016/J.NEUBIOREV.2011.12.013.

Nguyen, T, Schleihauf, H, Kayhan, E, Matthes, D, Vrticka, P, Hoehl, S, 2020. Neural synchrony in mother-child conversation: exploring the role of conversation patterns. Soc Cogn Affect Neurosci.

Overwalle, F.Van, 2009. Social cognition and the brain: a meta-analysis. Hum. Brain Mapp. 30, 829–858. doi:10.1002/hbm.20547.

Penny, W.D., Stephan, K.E., Mechelli, A., Friston, K.J., 2004. Comparing dynamic causal models. Neuroimage 22 (3), 1157–1172. doi:10.1016/j.neuroimage.2004.03.026.

Redcay, E., Schilbach, L., 2019. Using second-person neuroscience to elucidate the mechanisms of social interaction. Nat. Rev. Neurosci. 20 (8), 495–505. doi:10.1038/s41583-019-0179-4.

Řehůřek, R., Sojka, P., 2010. Software framework for topic modelling with large corpora. In: In Proceedings of the LREC 2010 Workshop on New Challenges for NLP Frameworks. University of Malta, pp. 46–50.

Rigoux, L., Stephan, K.E., Friston, K.J., Daunizeau, J., 2014. Bayesian model selection for group studies - revisited. Neuroimage 84, 971–985. doi:10.1016/j.neuroimage.2013.08.065.

Saito, D.N., Tanabe, H.C., Izuma, K., Hayashi, M.J., Morito, Y., Komeda, H., Sadato, N., 2010. Stay tuned: inter-individual neural synchronization during mutual gaze and joint attention. Front. Integr. Neurosci. (4) 1–12. doi:10.3389/fnint.2010.00127, NOVEMBER 2010.

Sammut, C., Webb, G.I, 2016. In: Sammut, C., Webb, G. (Eds.), Eds.. Springer US, Boston, MA.

Schilbach, L., 2010. A second-person approach to other minds. Nat. Rev. Neurosci. 11 (6). doi:10.1038/nrn2805-c1, 449–449.

Schilbach, L., 2014. On the relationship of online and offline social cognition. Front. Human Neurosci. 8, 278. doi:10.3389/fnhum.2014.00278, April.

Schilbach, L., Timmermans, B., Reddy, V., Costall, A., Bente, G., Schlicht, T., Vogeley, K., 2013. Toward a second-person neuroscience. Behav. Brain Sci. 36 (4), 393–414. doi:10.1017/S0140525X12000660.

Schmälzle, R., Brook O'Donnell, M., Garcia, J.O., Cascio, C.N., Bayer, J., Bassett, D.S., Falk, E.B., 2017. Brain connectivity dynamics during social interaction reflect social network structure. Proc. Natl. Acad. Sci. 114 (20), 5153–5158. doi:10.1073/pnas.1616130114.

Schmidt, C.F., Zaehle, T., Meyer, M., Geiser, E., Boesiger, P., Jancke, L., 2008. Silent and continuous fMRI scanning differentially modulate activation in an auditory language comprehension task. Hum. Brain Mapp. 29 (1), 46–56. doi:10.1002/hbm.20372.

Scholkmann, F, Holper, L, Wolf, U, Wolf, M, 2013. A new methodical approach in neuroscience: Assessing inter-personal brain coupling using functional near-infrared imaging (fNIRI) hyperscanning. Front Hum Neurosci 7.

Scholz, J., Triantafyllou, C., Whitfield-Gabrieli, S., Brown, E.N., Saxe, R., 2009. Distinct regions of right temporo-parietal junction are selective for theory of mind and exogenous attention. PLoS One 4 (3), e4869. doi:10.1371/journal.pone.0004869.

Schurz, M., Aichhorn, M., Martin, A., Perner, J., 2013. Common brain areas engaged in false belief reasoning and visual perspective taking: a meta-analysis of functional brain imaging studies. Front. Human Neurosci. 7, 1–14. doi:10.3389/fnhum.2013.00712, November.

Schurz, M., Radua, J., Aichhorn, M., Richlan, F., Perner, J., 2014. Fractionating theory of mind: a meta-analysis of functional brain imaging studies. Neurosci. Biobehav. Rev. 42, 9–34. doi:10.1016/j.neubiorev.2014.01.009.

Sebanz, N., Bekkering, H., Knoblich, G., 2006. Joint action: bodies and minds moving together. Trends Cogn. Sci. doi:10.1016/j.tics.2005.12.009.

Shaw, D., Czekóová, K., Gajdoš, M., Staněk, R., Špalek, J., Brázdil, M., 2019. Social decision-making in the brain: Input-state-output modelling reveals patterns of effective connectivity underlying reciprocal choices. Hum. Brain Mapp. 40 (2), 699–712. doi:10.1002/hbm.24446.

Shaw, D.J., Czekóová, K., Staněk, R., Mareček, R., Urbánek, T., Špalek, J., Brázdil, M., 2018. A dual-fMRI investigation of the iterated Ultimatum Game reveals that reciprocal behaviour is associated with neural alignment. Sci. Rep. 8 (1), 1–13. doi:10.1038/s41598-018-29233-9.

Shintel, H., Keysar, B., 2009. Less is more: a minimalist account of joint action in communication. Topics Cogn Sci 1 (2), 260–273. doi:10.1111/j.1756-8765.2009.01018.x.

Silbert, L.J., Honey, C.J., Simony, E., Poeppel, D., Hasson, U., 2014. Coupled neural systems underlie the production and comprehension of naturalistic narrative speech. Proceedings of the National Academy of Sciences of the United States of America 111 (43), E4687–E4696. doi:10.1073/pnas.1323812111.

Smittenaar, P., FitzGerald, T.H.B., Romei, V., Wright, N.D., Dolan, R.J, 2013. Disruption of dorsolateral prefrontal cortex decreases model-based in favor of model-free control in humans. Neuron 80. doi:10.1016/j.neuron.2013.08.009.

Špiláková, B., Shaw, D.J., Czekóová, K., Mareček, R., Brázdil, M., 2019. Getting into sync: data-driven analyses reveal patterns of neural coupling that distinguish among different social exchanges. Hum. Brain Mapp. 1–12. doi:10.1002/hbm.24861, November.

Stephan, K.E., Penny, W.D., Moran, R.J., den Ouden, H.E.M., Daunizeau, J., Friston, K.J., 2010. Ten simple rules for dynamic causal modeling. Neuroimage 49 (4), 3099–3109. doi:10.1016/j.neuroimage.2009.11.015.

Stephan, Klaas Enno, Penny, W.D., Daunizeau, J., Moran, R.J., Friston, K.J, 2009. Bayesian model selection for group studies. Neuroimage 46 (4), 1004–1017. doi:10.1016/j.neuroimage.2009.03.025.

Stephan, Klaas Enno, Weiskopf, N., Drysdale, P.M., Robinson, P.A., Friston, K.J, 2007. Comparing hemodynamic models with DCM. Neuroimage 38 (3), 387–401. doi:10.1016/j.neuroimage.2007.07.040.

Stephens, G.J., Silbert, L.J., Hasson, U., 2010. Speaker-listener neural coupling underlies successful communication. Proceedings of the National Academy of Sciences of the United States of America 10 (32), 14425–14430. doi:10.1073/pnas.1008662107.

Uddin, L.Q., Molnar-Szakacs, I., Zaidel, E., Iacoboni, M., 2006. rTMS to the right inferior parietal lobule disrupts self-other discrimination. Soc. Cogn. Affect. Neurosci. 1 (1), 65–71. doi:10.1093/scan/nsl003.

van Veluw, S.J., Chance, S.A., 2014. Differentiating between self and others: an ALE meta-analysis of fMRI studies of self-recognition and theory of mind. Brain Imaging Behav. 8 (1), 24–38. doi:10.1007/s11682-013-9266-8.

Vanlangendonck, F., Willems, R.M., Hagoort, P., 2018. Taking common ground into account : specifying the role of the mentalizing network in communicative language production. PLoS One 1–21. doi:10.1371/journal.pone.0202943.

Vossel, S., Geng, J.J., Fink, G.R., 2014. Dorsal and ventral attention systems: Distinct neural circuits but collaborative roles. Neuroscientist 20 (2), 150–159. doi:10.1177/1073858413494269.

Zadbood, A., Chen, J., Leong, Y.C., Norman, K.A., Hasson, U., 2017. How We Transmit Memories to Other Brains: Constructing Shared Neural Representations Via Communication. Cerebral Cortex 27 (10), 4988–5000. doi:10.1093/cercor/bhx202.

Zaehle, T., Schmidt, C.F., Meyer, M., Baumann, S., Baltes, C., Boesiger, P., Jancke, L., 2007. Comparison of “silent” clustered and sparse temporal fMRI acquisitions in tonal and speech perception tasks. Neuroimage 37 (4), 1195–1204. doi:10.1016/j.neuroimage.2007.04.073.

Zhang, S., Li, C.-S.R., 2013. Functional connectivity mapping of the human precuneus by resting state fMRI. Neuroimage 59 (4), 3548–3562. doi:10.1016/j.neuroimage.2011.11.023.Functional.